Mechanical and Physical Properties of Titanium Alloy Ti6Al4V-7Y

by

Mohamad Hanif Hazrin bin Md Zuki

Dissertation submitted in partial fulfillment of

the requirements for the

Bachelor of Engineering (Hons)

(Mechanical Engineering)

SEPTEMBER 2012

UniversitiTeknologi PETRONAS
Bandar Seri Iskandar
31750 Tronoh
Perak Darul Ridzuan

CERTIFICATION OF APPROVAL

Mechanical and physical properties of Titanium Alloy Ti6Al4V-7Y

by

Mohamad Hanif Hazrin bin Md Zuki

A project dissertation submitted to the
Mechanical Engineering Programme
UniversitiTeknologi PETRONAS
in partial fulfillment of the requirements for the
BACHELOR OF ENGINEERING (Hons)
(MECHANICAL ENGINEERING)

Approved by,

_____

(AP Dr. Patthi bin Hussain)

UNIVERSITI TEKNOLOGI PETRONAS
TRONOH, PERAK
SEPTEMBER 2012

CERTIFICATION OF ORIGINALITY

This is to certify that I am responsible for the work submitted in this project, that the original work is my own except as specified in the references and acknowledgements, and that the original work contained herein have not been undertaken or done by unspecified sources or persons.

_____

MOHAMAD HANIF HAZRIN BIN MD ZUKI

ABSTRACT

Ti6Al4V (grade 5) with different addition contents of wt.% yttrium (Y) element were fabricated successfully using FFC Cambridge process and the effects of Y content on the mechanical and physical properties of the alloys were investigated. Titanium alloy are broadly used in various application such as in the aerospace industries as bodies of aircraft and implants as in the biomechanical industries. The objectives of this project are to determine the mechanical and physical properties of Ti6Al4V-7Y and to identify the effect of different addition contents of wt.% Y element in the alloy. In order to determine the physical properties of Ti6Al4V-7Y, the sample was put in Variable Pressure-Field Emission Scanning Electron Microscope (VP-FESEM), X-ray Diffraction (XRD) machine and optical microscope. While Vickers Hardness tester was used to determine the mechanical properties of the alloy. The result shows that Ti6Al4V-7Y has bigger grain size than Ti6Al4V-2Y and the hardness value of Ti6Al4V-7Y is smaller than Ti6Al4V-2Y. It was observed that Ti6Al4V-7Y has porous surface. On the other hand, the diffraction peak intensities of Y_2O_3 phases increased with the increasing of Y content. As conclusion, the mechanical and physical properties of Ti6Al4V-7Y and the effect of different addition contents of wt.% Y element in the alloy have been investigated successfully.

ACKNOWLEDGEMENT

First and foremost, I would like to take this opportunity to express my greatest appreciation to my Final Year Project supervisor, AP Dr. Patthi Hussain for his valuable guidance and advices throughout my entire project. His supports, patience, and willingness to assist me in the problem or difficulties that I faced in my project have contributed tremendously to my project. I also wish to take this opportunity to express my utmost gratitude to the individual and parties that have contributed their time and efforts in assisting me to complete this project, directly or indirectly. Without their helps and assistances, there is no doubt that I would face some difficulties throughout the whole project. This project would not be in success without all of their supports, guidance and patience. I also would like to take this opportunity to thank the Final Year Project coordinator, Dr. Hasan Fawad for his effort in ensuring the project is progressed smoothly within the time frame given. Last but not least, I would like to give my utmost gratitude and appreciation to my family and fellow friends for their support and inspiration so that this project can be completed successfully.

TABLE OF CONTENTS

LIST OF FIGURES

LIST OF TABLES

CHAPTER 1

1. INTRODUCTION

1.1 Project Background

There are many metals produced by reduction of their own oxides. The reduction can be achieved by using different type of process while taking into account relative stability of metal oxides and the oxides of impurities [1]. Reduction of relatively unstable oxides can be conducted by producing the heat until their decomposition temperature (eg. HgO) but the most common reductant is carbon (FeO). Although carbon can be used to reduce almost all metal oxide, very high temperatures are needed to accomplish the reduction which brings problem such as difficulty in stopping the back reaction (MgO) or the formation of stable carbides (Ti_2O). In addition, electrolysis of aqueous or more commonly known as molten salt solution can be used to dissolve the metal oxides. For compounds that are very stable such as (Al_2O_3), fused salt electrolysis the best way but this technique is suitable for metals that are deposited in the melting point of the metal is less than reduction temperature of its oxide (Al) [1]. For high melting point of metal (Ti), it is basically difficult to hold out molten salt electrolysis. Furthermore, (Ti) was always polluted with significant amount of oxygen. In recent times, the FFC Cambridge process was possible to reduce solid oxide films on titanium foil by making the foil cathodic in a bath of molten calcium chloride and it is also possible to reduce solid titanium oxide pellets. In addition, this process is not only for titanium dioxide but other metal oxides as well.

1.2 Problem Statement

This project starts with pinning of yttrium into titanium alloy, Ti6Al4V. Yttrium is a soft, silver-metallic, lustrous and highly crystalline transition metal in group 3. 7 wt.% of yttrium will be added into the alloy by using FFC Cambridge process. The pinning action is expected to reduce the grain size of titanium alloy and further improving the strength [2]. The pinning of yttrium to titanium alloy will affected the hardness value, workability, and grain size. In this project, we will utilize the concept of

determining hardness on a specific material. Vickers Hardness Test plays a massive role in order to determine the value of hardness of the alloy used, which in this case is Ti6Al4V with added 7 wt.% Y. The Vickers Hardness Test is regularly easier to use than other hardness tests since the required calculations are independent of the size of the indenter. Besides, the indenter can be used for all materials regardless of hardness. The basic principle, as with all communal measures of hardness, is to discern the questioned material's ability to resist plastic deformation from a given source. The Vickers Hardness Test can be used for all metals and has one of the broadest scales among hardness tests. The unit of hardness specified by the test is known as the Diamond Pyramid Hardness (DPH) or the Vickers Pyramid Number (HV). The hardness number is determined by the load over the surface area of the indentation and not the area normal to the force, and is therefore not a pressure. The hardness number is not really a true property of the material and is an empirical value that should be seen in unification with the experimental methods and hardness scale used. Various Pressure-Field Emission Scanning Electron Microscope (VP-FESEM) and Optical Microscope will determine the microstructure of Ti6Al4V-7Y while X-ray Diffraction (XRD) test will determine the composition of Ti6Al4V-7Y.

1.3 Objectives

The objective of this research work is to determine the mechanical and physical properties on the effect of addition 7 wt.% Y in Ti6Al4V alloy via FFC process.

1.4 Scope of study

This work is actually a laboratories-based project in which it emphasizes the engineering knowledge and analyzing the problem by means of practical laboratories work so that physical and mechanical properties of Ti6Al4V-7Y under certain condition can be obtained. This project focus on the ability to understand the problem encountered and to use the entire necessary test needed in order to verify the feasibility and reliability of the proposed solution of the problem. In this case, the problem is to determine the physical and mechanical properties of Ti6Al4V-7Y. In order to verify its physical

properties, the sample was observed under the Optical Microscope and Scanning Electron Microscope (SEM). X-ray Diffraction test was conducted to determine the orientation of a single crystal or grain and find the crystal structure of Ti6Al4V-7Y. It is also to measure the average spacing between layers or row of atoms, size, shape and internal stress of its regions. As for mechanical properties, Vickers Hardness Test was conducted to determine the yield strength.

CHAPTER 2

2. LITERATURE REVIEW

2.1 Effect of β grain growth in Ti6Al4V

G.C Obasi [3] had been investigated the texture evolution and the role of β grain growth on alternate selection during β - α phase transformation had been examined in Ti6Al4V with and without addition of 0.4 wt.% yttrium (Y). The purpose of adding yttrium was to control β grain growth above the β transus by pinning grain boundaries with yttria. Both materials had been conducted by thermo mechanically process to generate related crystallographic textures and starting microstructures. Furthermore, both materials were solution-heat-treated above the β transus followed by slow cooling to encourage growth of the α lath structure from grain boundary α. Extra interrupted slow cooling experiments had been carried out to classify the α lamellae that nucleate first from β grain boundaries. Complete electron backscatter diffraction analysis had been carried out and it was found that the β heat treatment did not generate new texture components even though the intensities of the individual components changed significantly depending on the alloy β grain size. Alternate selection was assessed by comparing measured α texture components with predicted α texture components based on the high-temperature β texture assuming equal alternate selection. It was found that with increasing β grain size variant selection intensified favoring the {φ 1, φ, φ 2} {90˚, 30˚, 0˚} texture component. Interrupted cooling experiments revealed that α nucleates first on b grain boundaries that are formed by two b grains having a common (110) normal and that these α lamellae display almost exclusively a {φ1, φ, φ 2} {90˚, 30˚, 0˚} orientation. As a result, the power of this variant with increasing β grain size can be linked to the relative free growth of this particular α texture component into an “empty” β grain. Figure 2.1 and Figure 2.2 show optical micrograph of recrystallized and β heat-treated samples. Figure 2.3 shows the β grain size distributions of sample after β heat treatment.

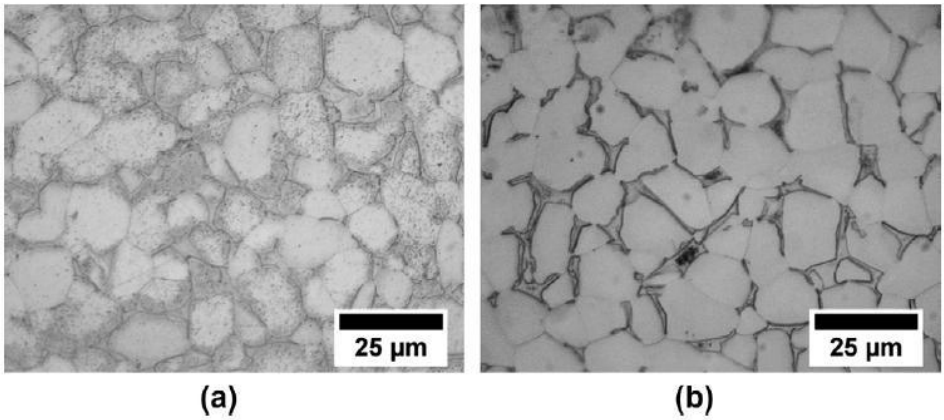

Figure 2.1: Optical micrographs of sample recrystallized (RX) at 950 ˚C for 8 hours: (a) Ti6Al4V and (b) Ti6Al4V-0.4Y [3]

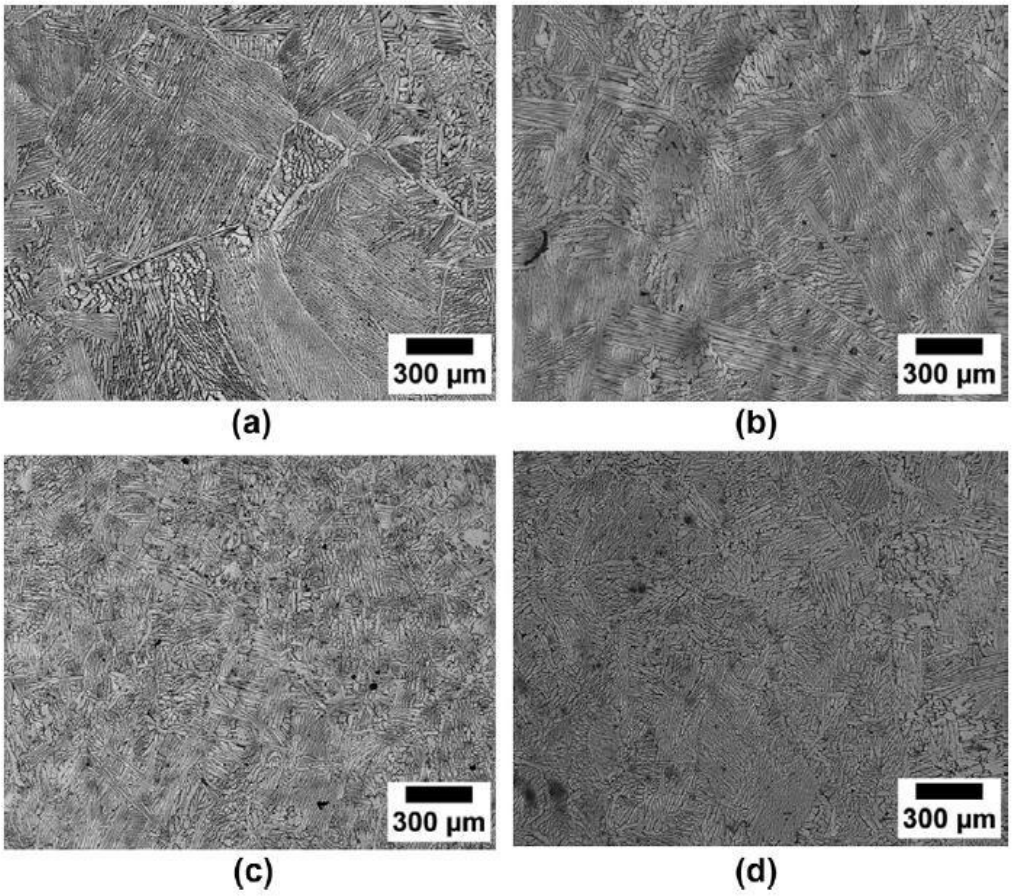

Figure 2.2: Optical micrograph of β heat-treated samples: (a) Ti-6Al-4V at 1050 ˚C (b) Ti6Al4V at 1150 ˚C (c) Ti6Al4V-0.4Y at 1050 ˚C (d) Ti6Al4V-O.4Y at 1150 ˚C [3].

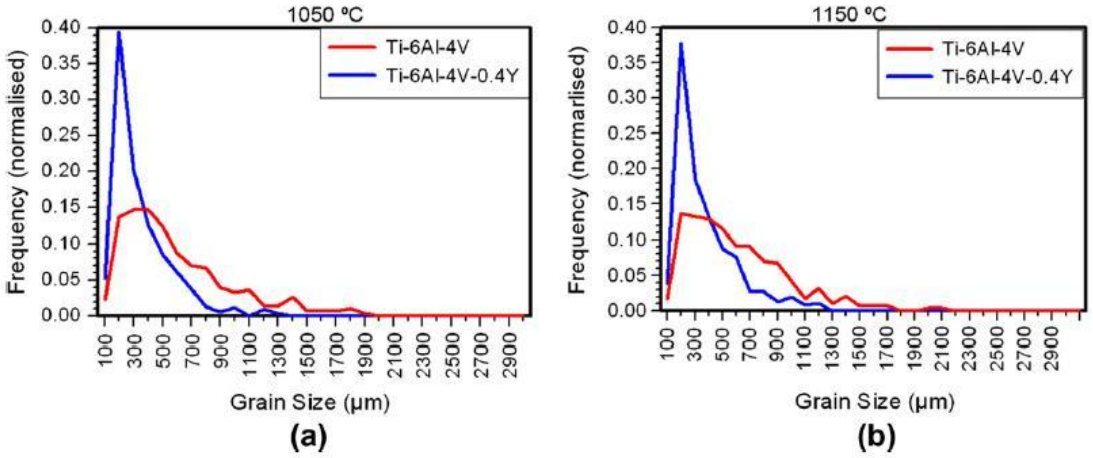

Figure 2.3: The β grain size distributions of samples after β heat treatment: (a) Ti6Al4V and Ti6Al4V-0.4Y at 1050 ˚C (b) Ti6Al4V and Ti6Al4V-0.4Y at 1150 ˚C [3].

In Figure 2.1, optical micrographs of Ti6Al4V show after recrystallizing the material at 950 ˚C for 8 hours will reveal in both cases a fully equiaxed primary a microstructure with a mean grain size of 18 μm and retained β at the triple junctions of primary α (α_p). The likeness of the grain morphology and the α textures in both alloys show that yttrium additions did not have any significant effect on the microstructure produced during thermomechanical processing. In addition, an almost look alike starting microstructure was achieved between two alloys before receiving any β heat treatment for variant selection of studies. We can see in Figure 2.3 that Ti6Al4V shown a wider grain size distribution compares to Ti6Al4V-0.4Y for both temperatures with a significant tail towards grain sizes exceeding 1mm. While in Figure 2.2, β grains of Ti6Al4V are easily recognized by continuous film of grain boundary α (α_{GB}). Meanwhile, Ti6Al4V-0.4Y grain boundary α was less distinct [3].

2.2 Ti6Al4V Titanium Alloys

2.2.1 General characteristics

Titanium alloy have high strength, low weight ratio and outstanding corrosion resistance. That's why it has been used in a wide range of successful applications which demand high levels of consistent routine in medical as well as in aerospace, automotive, chemical plant, and other major industries. In addition, titanium has replaced heavier, less serviceable or less cost effective materials. Designing with titanium while consider all factors into account has resulted in consistent, economic and more durable systems or components. There are many different grade of titanium available. Ti6Al4V is defines as grade 5. It is the most frequently used alloy and stronger than pure titanium but have same stiffness and thermal properties. Furthermore, it is heat treatable. This grade is an outstanding mixture of strength, resistance of corrosion, weld and fabric-ability. Therefore, it is used broadly in wide range of major industries.

2.2.2 Special characteristics

Ti6Al4V is the most common used titanium alloy. It features good machine-ability and excellent mechanical properties. The Ti6Al4V alloy offers the excellent performance for a multiple of weight reduction applications in major industries. It is also has numerous applications in the medical industry and has excellent biocompatibility [4].

2.2.3 Applications

Ti6Al4V is typically used for [4]:

- Direct Manufacturing of parts and prototypes for racing and aerospace industry
- Biomechanical applications, such as implants and prosthesis
- Marine applications
- Chemical industry

a **CHEMICAL SPECIFICATION**

	Arcam Ti6Al4V, Typical	Ti6Al4V, Required*	Ti6Al4V, Required**
Aluminium, Al	6%	5,5–6,75%	5,5–6,75%
Vanadium, V	4%	3,5–4,5%	3,5–4,5%
Carbon, C	0,03%	< 0,1%	< 0,08%
Iron, Fe	0,1%	< 0,3%	< 0,3%
Oxygen, O	0,15%	< 0,2%	< 0,2%
Nitrogen, N	0,01%	< 0,05%	< 0,05%
Hydrogen, H	0,003%	< 0,015%	< 0,015%
Titanium, Ti	Balance	Balance	Balance

*ASTM F1108 (cast material) **ASTM F1472 (wrought material)

b **MECHANICAL PROPERTIES**

	Arcam Ti6Al4V, Typical	Ti6Al4V, Required**	Ti6Al4V, Required***
Yield Strength (Rp 0,2)	950 MPa	758 MPa	860 MPa
Ultimate Tensile Strength (Rm)	1020 MPa	860 MPa	930 MPa
Elongation	14%	>8%	>10%
Reduction of Area	40%	>14%	>25%
Fatigue strength* @ 600 MPa	>10,000,000 cycles		
Rockwell Hardness	33 HRC		
Modulus of Elasticity	120 GPa		

*After Hot Isostatic Pressing **ASTM F1108 (cast material) ***ASTM F1472 (wrought material)

The mechanical properties of materials produced in the EBM process are comparable to wrought annealed materials and are better than cast materials.

Figure 2.4: (a) Chemical specification comparison between Arcam Ti6Al4V, cast Ti6Al4V and wrought Ti6Al4V and (b) Mechanical properties comparison between Arcam Ti6Al4V, cast Ti6Al4V and wrought Ti6Al4V [4].

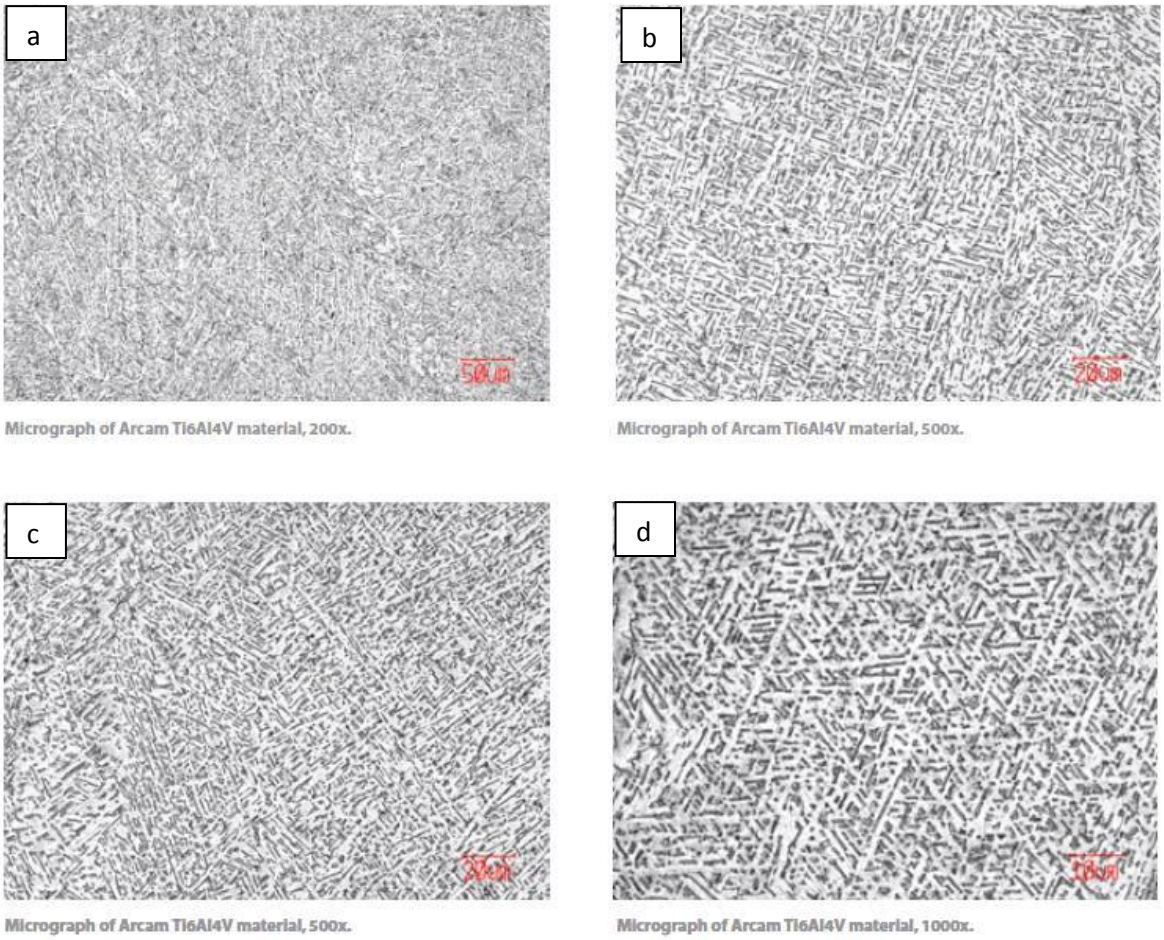

Figure 2.5: Micrograph of Arcam Ti6Al4V material: (a) 200X zoom, (b) 500X zoom, (c) 500X zoom and (d) 1000X zoom [4].

Arcam [4] said that their Ti6Al4V parts manufactured in the EBM process have a microstructure better than cast Ti6Al4V containing a lamellar α-phase with larger β-grains, and with a higher density and significantly finer grain, thanks to the rapid cooling of the melt pool. The build chamber is kept at an elevated temperature throughout the entire build, and the material thus comes out of the EBM process in a naturally aged condition.

2.3 Hydrogen Embrittlement of Aluminium

Lu proposed [5] four general mechanism; (i) formation of a hydride phase; (ii)enhanced local plasticity; (iii) grain boundary weakening and(iv) blister and bubble formation. For these mechanisms to be operational, however, a critical local concentration of H is required, either to form a hydride phase or to initiate cracking at microvoids and grain boundaries. One of the outstanding problems in the current theories of hydrogen embrittlement is the lack of a comprehensive and coherent atomistic mechanism to account for the critical H concentrations at crack tips. Moreover, it is widely observed that H-enhanced dislocation mobility is a prelude to the embrittlement and the fracture planes coincide with the slip plane of the material, which is not the typical situation; how all these phenomena come about still remains a mystery. It is generally believed that dislocations are central to H embrittlement phenomena, and a large body of work has been dedicated to elucidate hydrogen-dislocation interaction and its consequences on embrittlement. Vacancies, being universally present in solids and having the ability to act as impurity traps could play a central role in the embrittlement process, but detailed arguments about this role or estimates of its relative importance are totally lacking.

2.4 Vickers Hardness Test

According to Instron [10], Vickers test methods are defined in the following standards:

- ASTM E384 – micro force ranges – 10g to 1kg
- ASTM E92 – macro force ranges - 1kg to 100kg
- ISO 6507-1,2,3 – micro and macro ranges

All Vickers ranges use a 136° pyramidal diamond indenter that forms a square indent [10].

- The indenter is pressed into the sample by an accurately controlled test force.

- The force is maintained for a specific dwell time, normally 10 – 15 seconds.
- After the dwell time is complete, the indenter is removed leaving an indent in the sample that appears square shaped on the surface.
- The size of the indent is determined optically by measuring the two diagonals of the square indent.
- The Vickers hardness number is a function of the test force divided by the surface area of the indent. The average of the two diagonals is used in the following formula to calculate the Vickers hardness.

HV = Constant x test force / indent diagonal squared

Because of the wide test force range, the Vickers test can be used on almost any metallic material. The part size is only limited by the testing instrument's capacity [10].

Strengths

1. One scale covers the entire hardness range. A wide range of test forces to suit every application Nondestructive, sample can normally be used.

Weaknesses

1. The main drawback of the Vickers test is the need to optically measure the indent size. This requires that the test point be highly finished to be able to see the indent well enough to make an accurate measurement.
2. Slow. Testing can take 30 seconds not counting the sample preparation time.

`

Figure 2.6: Vickers Hardness Tester Machine

2.5 X-ray Diffraction

According to pdx [11], X-ray diffraction techniques are a non-destructive test which reveals information about the crystal structure, chemical composition, and physical properties of materials and thin films. These techniques are based on observing the scattered intensity of an X-ray beam hitting a sample as a function of incident beam that will be diffracted and transmitted. The diffraction pattern will be recorded.

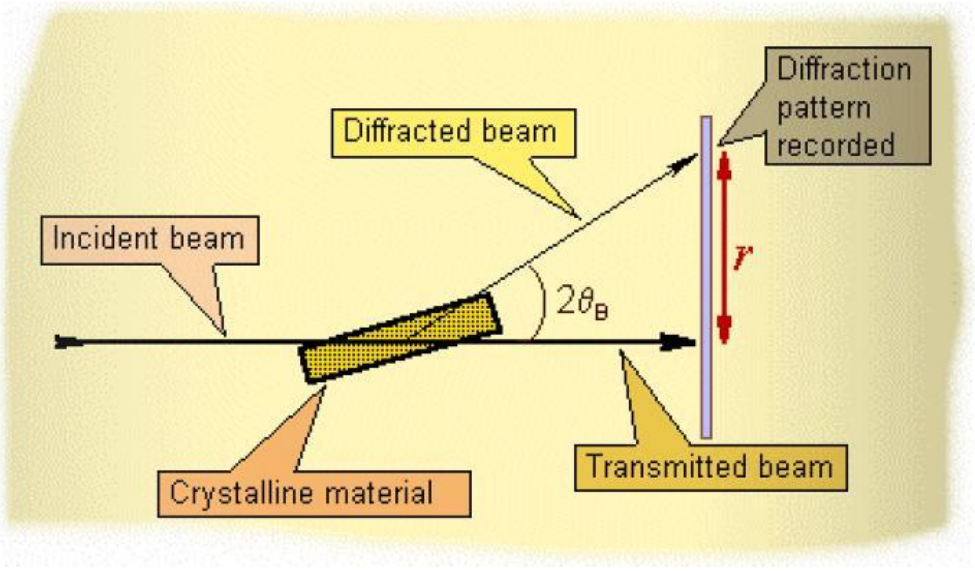

Figure 2.7: Operation of X-ray Diffraction [11].

2.5.1 Implementation

XRD users must be trained in operation and basic radiation safety in order to use the XRD machine. There are strictly no exceptions to ignore this rule. In Universiti Teknologi Petronas (UTP), students did not have the qualification to use the XRD machine. The entire test will be conducted by technician who has the authority to use the machine. Basically, there are 3 steps to use XRD machine which are sample preparation, XRD log and operation.

2.6 Phase identification of Y addition on TiC/Ti6Al4V composites

According to Wang [13], The X-ray diffraction (XRD) analysis of Ti6Al4V alloy and TiC/Ti6Al4V composites with different Y element contents are shown in Figure 8. It is show that, Ti6Al4V alloy mainly consists of α-Ti phase. Furthermore, it is known that α-Ti is the original solidification phase of Ti6Al4V alloy. For the composites without Y element and with 0.1 wt.% of Y element, only α-Ti and TiC appeared, nevertheless, at certain points, content of Y element resulted in a new compound of Y_2O_3. The diffraction peak intensities of Y_2O_3 phases increased with the increasing of Y content, which indicated Y_2O_3 phase content increased steadily. Formation of Y_2O_3 might be increased by the use of argon atmosphere containing O_2. Wang said [13], the solid solubilities of Y in β-Ti and α-Ti are less than 0.1% and 0.2%, correspondingly, but there is no compound formation between Ti and Y. Meanwhile. On the other hand, the solid solubility of Y in Al is near to zero and the solid solubility of Y in TiAl based alloy was very limited, even in the rapidly solidified alloys. Wang [13] also said that adding Y to TiAl alloys could result in the formation of Y_2O_3. Normally, the rare earth elements can react with many elements to form compounds due to their vigorous chemical properties and the binding force among atoms increases with increasing electro negativity difference [13].

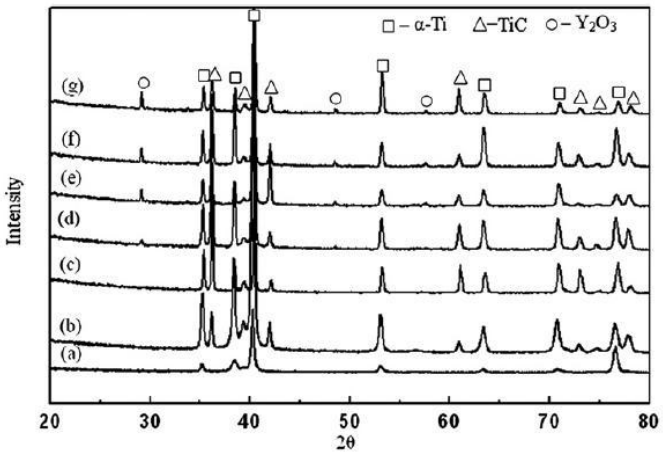

Figure 2.8: XRD results of TiC/Ti6Al4V composites with different Y element contents. (a) Ti6Al4V. (b) TiC/Ti6Al4V. (c) TiC/Ti6Al4V + 0.1Y. (d) TiC/Ti6Al4V + 0.3Y. (e) TiC/Ti6Al4V + 0.5Y. (f) TiC/Ti6Al4V + 1.0Y. (g) TiC/Ti6Al4V + 2.0Y [13].

CHAPTER 3

3. METHODOLOGY

3.1 Planned progress flow of the project

In this study, various laboratories works have been conducted to obtain physical and mechanical properties of Ti6Al4V-7Y. In order to achieve the objectives with data collection and comparison study, the experimental procedure was conducted with the incorporation of facilities and equipments which are provided by Mechanical Engineering Department, Universiti Teknologi PETRONAS. This chapter focused on the planned progress flow for this project. After the project title was selected, a preliminary research work was done including consultation with the supervisor to get the overview and basic understanding of the selected project. The details, samples and information of the project which was given by the supervisor have been studied in order to understand the project background, problem statement, objectives and scope of study for this particular project. The samples were acquired by FFC Cambridge process. After fully understand the basics of the project, a more thorough research work was done for the literature review of this project. During this stage, all related materials and information including the previous researches and journals were retrieved as much as possible for a more thorough and deep understanding on the mechanical and physical properties of Ti6Al4V-7Y. Then, after all the research works have been completed, the main stage of this project was initiated. Firstly, in order to determine the physical properties of Ti6Al4V-7Y the sample was put in Variable Pressure-Field Emission Scanning Electron Microscope (VP-FESEM) manufactured by Carl Zeiss AG, Germany, (SUPRA55VP model) and optical microscope. Field Emission Scanning Electron Microscope with ultra high resolution imaging is designed to fulfill the requirements of analyzing up to nano scale surface structure and morphology of solids. A well-defined electron beam impinges on the specimen and leads to generation of secondary electrons, back scattered electrons, absorbed electron and characteristic X-ray. These electrons can be detected by suitable detectors and give information about the surface structure and morphology of the specimens. The characteristic X-rays generated are used for

identification of different elements present in the specimen by energy dispersive spectrometer (EDS). With various pressure modes, non-conducting samples can be imaged without prior preparation. After completing those tests, phase identification was carried out via X-ray Diffraction (XRD) in order to analyze the diffraction pattern. All specimens were prepared to powder form in order to inspect them. After each diffraction patterns have been acquired, patterns were examined whether new peak was formed or was there any peak loss within the new pattern of Ti6Al4V-7Y.In order to determine mechanical properties of the alloy, Vickers hardness test was conducted by using dwell time of 15 seconds and load of 1000gf. When all tests had been completed, the results obtained were discussed and analyzed in order to verify mechanical and physical properties of Ti6Al4V-7Y. The results obtained from the tests have determined the morphology; element distribution and phase identification of Ti6Al4V-7Y. Figure 3.1 shows the steps taken flow for this project.

3.2 Project flow chart of the steps taken

Project flow shows the steps taken to determine mechanical and physical properties of Ti6Al4V-7Y.

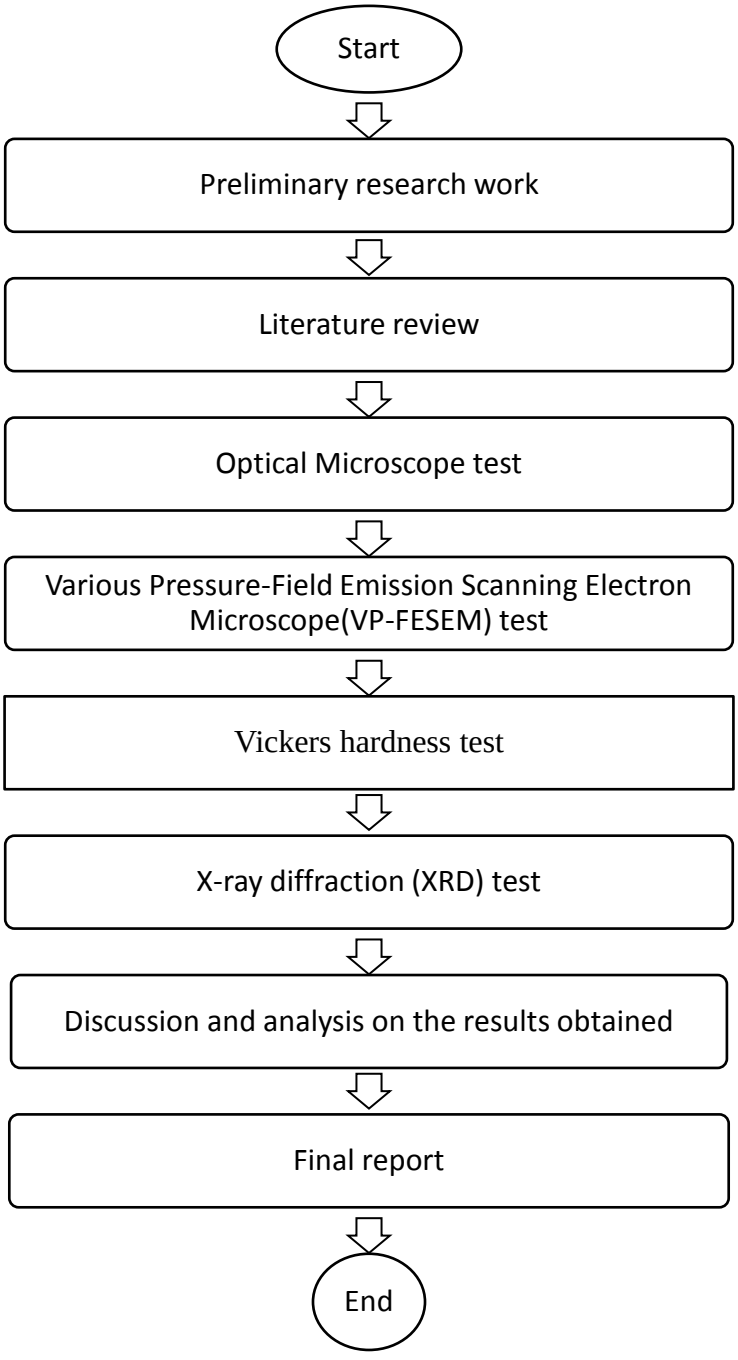

Figure 3.1: Project flow chart of the steps taken

3.3 Project timeline

Table 3.1: Project Activities and Key Milestones for FYP I

No.	Detail/ Week	1	2	3	4	5	6	7		8	9	10	11	12	13	14
1	Selection of Project Topic	■														
									M							
2	Preliminary Research Work		■	■	■	■	■		**I**							
									D							
3	Submission of Extended Proposal							○	**S**							
									E							
4	Proposal Defense								**M**		○					
									B							
5	Execution of project								**R**			■	■	■	■	
									E							
6	Submission of Interim Draft Report								**A**						○	
									K							
7	Submission of Interim Report															○

Legends:

■ Project Activity

○ Key Milestone

Table 3.2: Project Activities and Key Milestones for FYP II

No.	Detail/ Week	1	2	3	4	5	6	7		8	9	10	11	12	13	14	15
1	Project work	■	■	■	■	■	■	■									
2	Submission of progress report									●							
									MID								
3	Project work continues									■	■	■					
									SEM								
4	Submission of Draft report													●			
									BREAK								
5	Submission of dissertation(soft bound)														●		
6	Submission of Technical paper														●		
7	VIVA															●	
8	Submission of dissertation(hard bound)																●

Legends:

■ Project Activity

● Key Milestone

CHAPTER 4

4. RESULT AND DISCUSSION

4.1 Data gathering

This project consisted of two main parts; the mechanical and the physical properties of Ti6Al4V-7Y. Physical properties can be obtained by Optical Microscope, Various Pressure-Field Emission Scanning Electron Microscope (VP-FESEM) and X-ray Diffraction (XRD) machine. While mechanical properties can be obtained by Vickers Hardness Test.

4.2 Microstructures

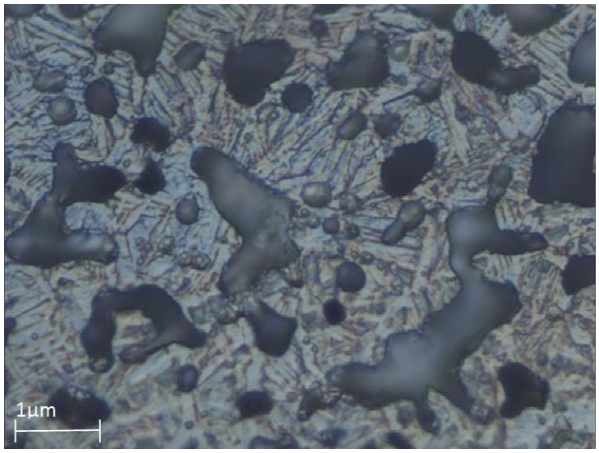

Figure 4.1: Microstructures of Ti6Al4V-7Y using optical microscope : at 150x magnification

From Figure 4.1, micrographs of Ti6Al4V-7Y are similar as in the literature review of Arcam Ti6Al4V [4] but Ti6Al4V-7Y has porosities due to it's proposed for biomedical applications [12] by FFC Cambridge process. By conducting Vickers hardness test, the average hardness of Ti6Al4V-7Y is **156.1 HV** while Ti6Al4V-2Y is **161.7 HV** by using dwell time of 15 seconds and load of 1000gf. The Arcam Ti6Al4V [4] from literature review has better hardness than Ti6Al4V-7Y and Ti6Al4V-2Y

because both of them have porosities. Porosity is reported to lower the hardness and tensile strength of the material [12].

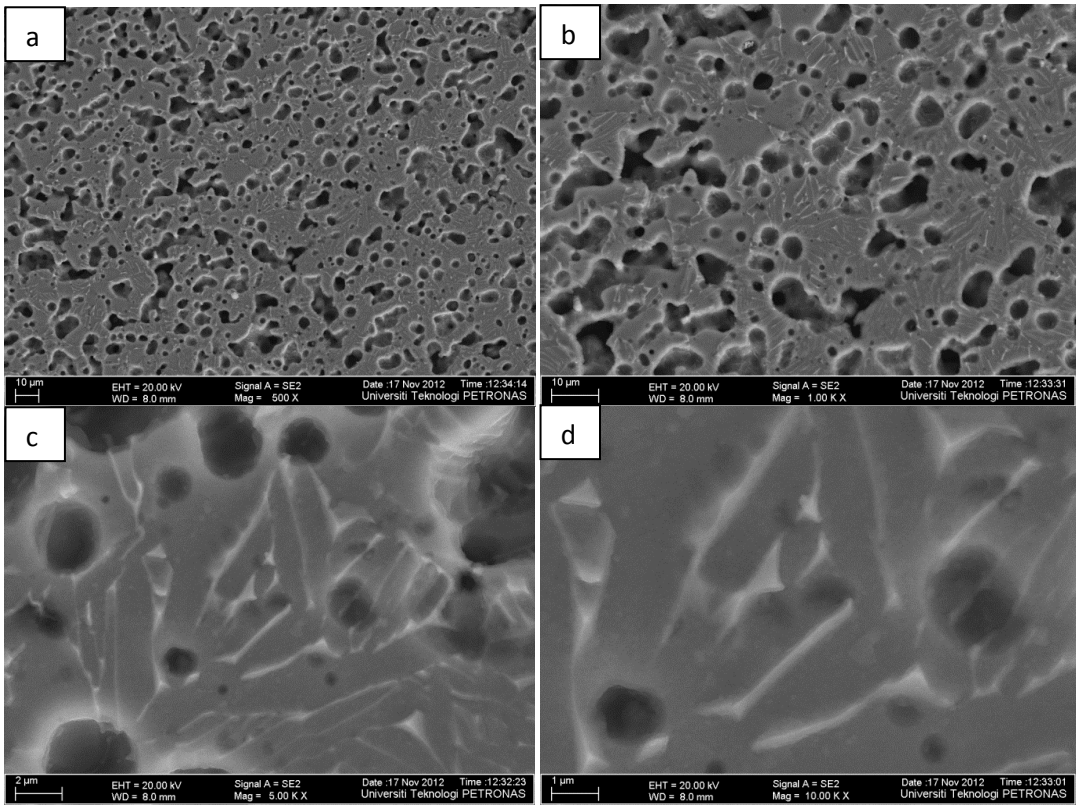

Figure 4.2: Microstructures of Ti6Al4V-7Y using VP-FESEM : a) 500x magnification b) 1000x magnification c) 5000x magnification d) 10000x magnification.

From Figure 4.2, the microstructure of Ti6Al4V-7Y consisted of two parts which are lighter and darker area. Lighter area is the grain boundaries of Ti6Al4V-7Y and darker area is the porosity located on Ti6Al4V-7Y. The advantage of porosity in Ti6Al4V-7Y is to lower the strength and satisfy the strength requirements for bone replacement in biomedical application [12]. Figure 4.3 shows that the comparison of Ti6Al4V-7Y grain boundaries and Ti6Al4V-2Y grain boundaries. There are many techniques to determine the grain size. One of the simplest techniques to approximate an average grain size is the intercept technique. First, a random straight line is drawn through the micrograph. The numbers of grain boundaries intersecting the line are counted. The average grain size is determined by dividing the number of intersections by the actual line length.

Average grain size =1/(number of intersections/actual length of the line).

where actual line length = measured length divided by magnification

From this formula, three random straight lines are drawn through the micrograph to get average grain size of Ti6Al4V-7Y and Ti6Al4V-2Y at 5000x magnification. The result for average grain size of Ti6Al4V-7Y is **2.53µm** and average grain size of Ti6Al4V-2Y is **1.44µm**.

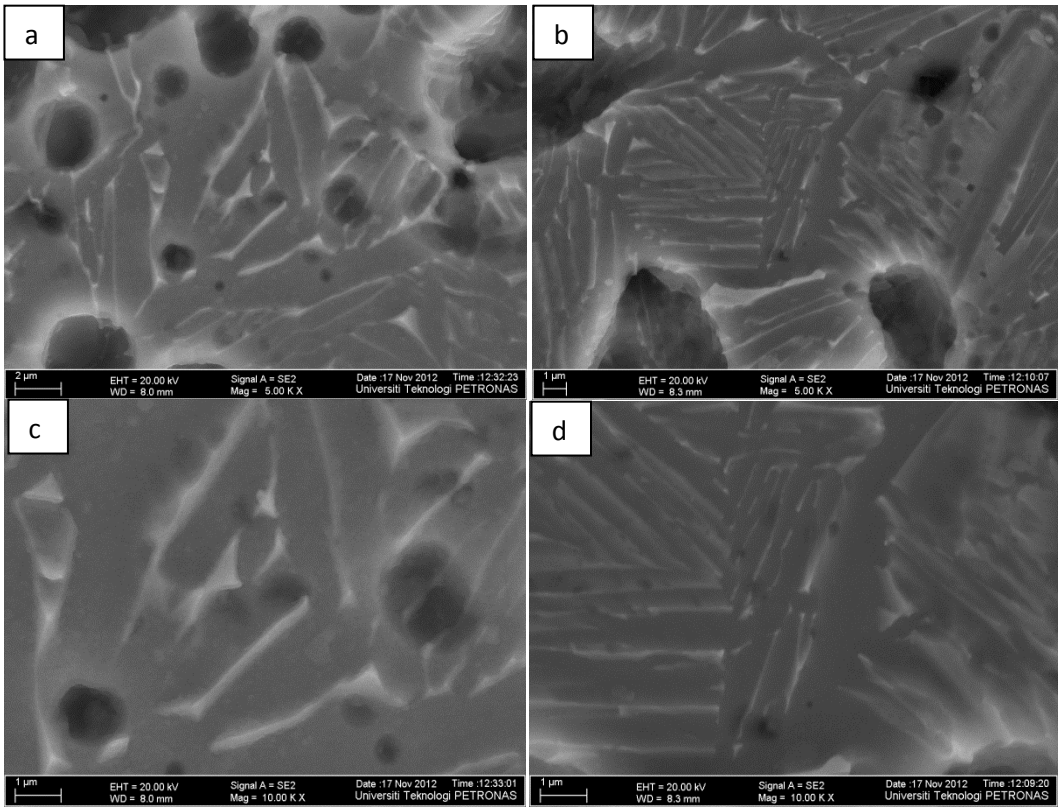

Figure 4.3: Comparison between grain boundaries of Ti6Al4V-7Y and Ti6Al4V-2Y : a) Ti6Al4V-7Y at 5000x b) Ti6Al4V-2Y at 5000x c) Ti6Al4V-7Y at 10000x d) Ti6Al4V-2Y at 10000x.

4.3 Energy Dispersive X-ray analysis (EDX)

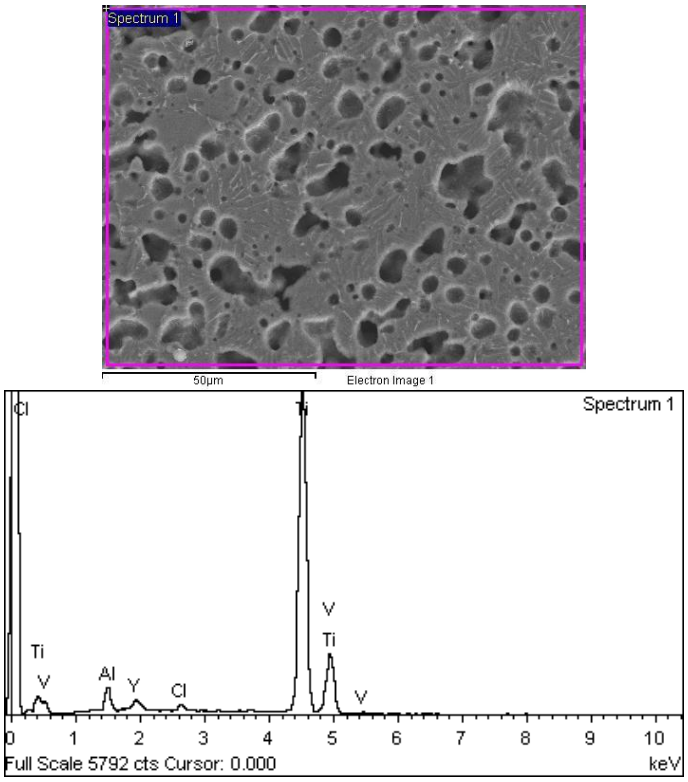

Figure 4.4: EDX analysis at spectrum 1

Table 4.1: Elements distribution of Ti6Al4V-7Y at spectrum 1.

Element	Weight %	Atomic %
Ti	88.03	86.99
Al	3.37	5.91
V	4.89	4.55
Y	2.98	1.59
Cl	0.72	0.97

Figure 4.4 shows that the EDX analysis at spectrum 1 which is overall area on micrograph of Ti6Al4V-7Y at 1000x magnification. Results from Table 4.1 shows that

Ti element has the most weight percentage follow by V, Al, Y and Cl element. Cl element is believed comes from the FFC Cambridge process [1].

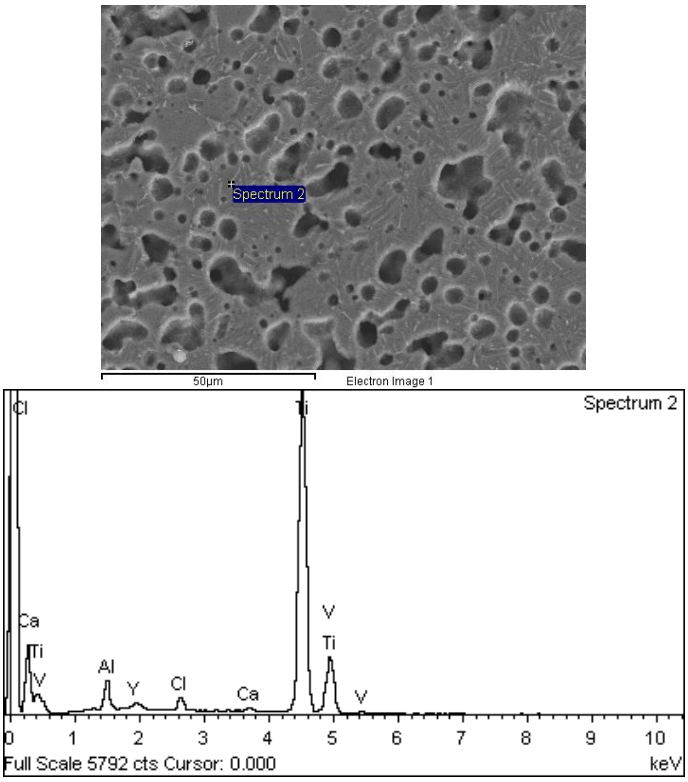

Figure 4.5: EDX analysis at spectrum 2

Table 4.2: Elements distribution of Ti6Al4V-7Y at spectrum 2.

Element	Weight %	Atomic %
Ti	86.86	84.55
Al	4.08	7.06
V	4.72	4.32
Y	1.94	1.02
Cl	1.78	2.35
Ca	0.61	0.71

Figure 4.5 shows that the EDX analysis at spectrum 2 which is at the grain boundaries area on micrograph of Ti6Al4V-7Y at 1000x magnification. Results from Table 4.2 shows that Ti element has most weight % follow by V, Al, Y, Cl and Ca element. Cl and Ca elements are believed come from the FFC Cambridge process as its electrolyte [1].

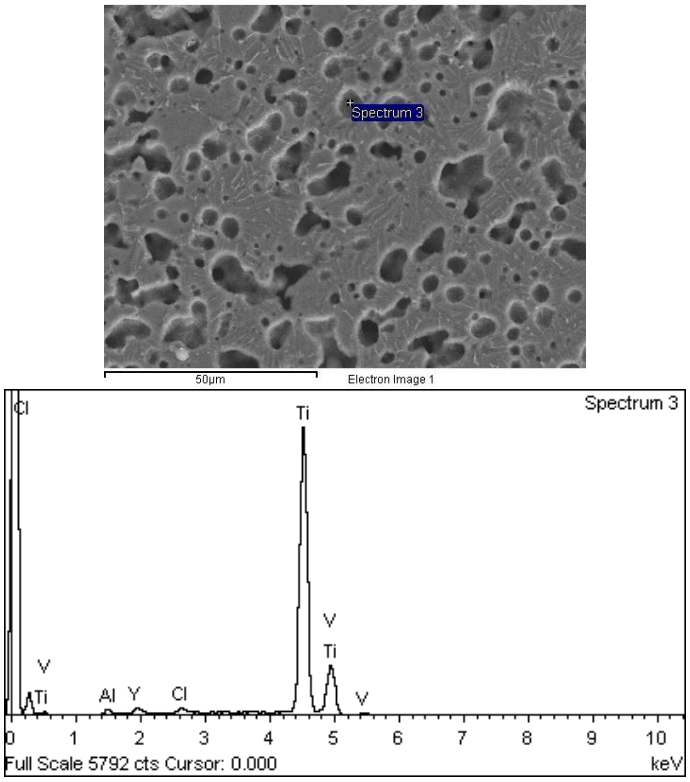

Figure 4.6: EDX analysis at spectrum 3

Table 4.3: Elements distribution of Ti6Al4V-7Y at spectrum 3.

Element	Weight %	Atomic %
Ti	91.59	91.90
Al	0.93	1.65
V	4.56	4.30
Y	2.24	1.21
Cl	0.69	0.94

Figure 4.6 shows that the EDX analysis at spectrum 3 which is at the porosity / darker area on micrograph of Ti6Al4V-7Y at 1000x magnification. Results from Table 4.3 shows that Ti element has most weight percentage follow by V, Y, Al, and Cl element. From results of Table 4.2 and Table 4.3, they showed that Y element is mainly at the porosity area of Ti6Al4V-7Y and less at the grain boundaries area of Ti6Al4V-7Y.

4.4 Mapping

4.4.1 Ti6Al4V-7Y elements mapping

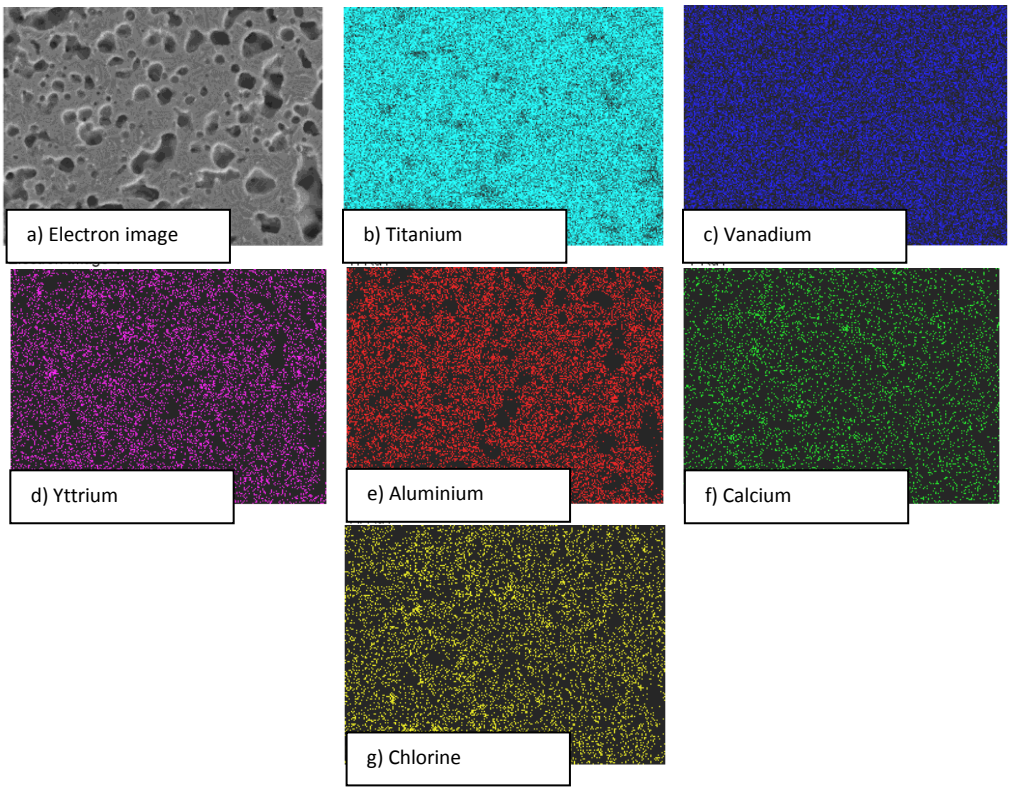

Figure 4.7: Elements mapping of Ti6Al4V-7Y.

From Figure 4.7, all elements of Ti6Al4V-7Y are well distributed across of the sample. It was found that Y element is located mainly at the grain boundaries and less located at the porous area of the sample.

4.4.2 Ti6Al4V-2Y elements mapping

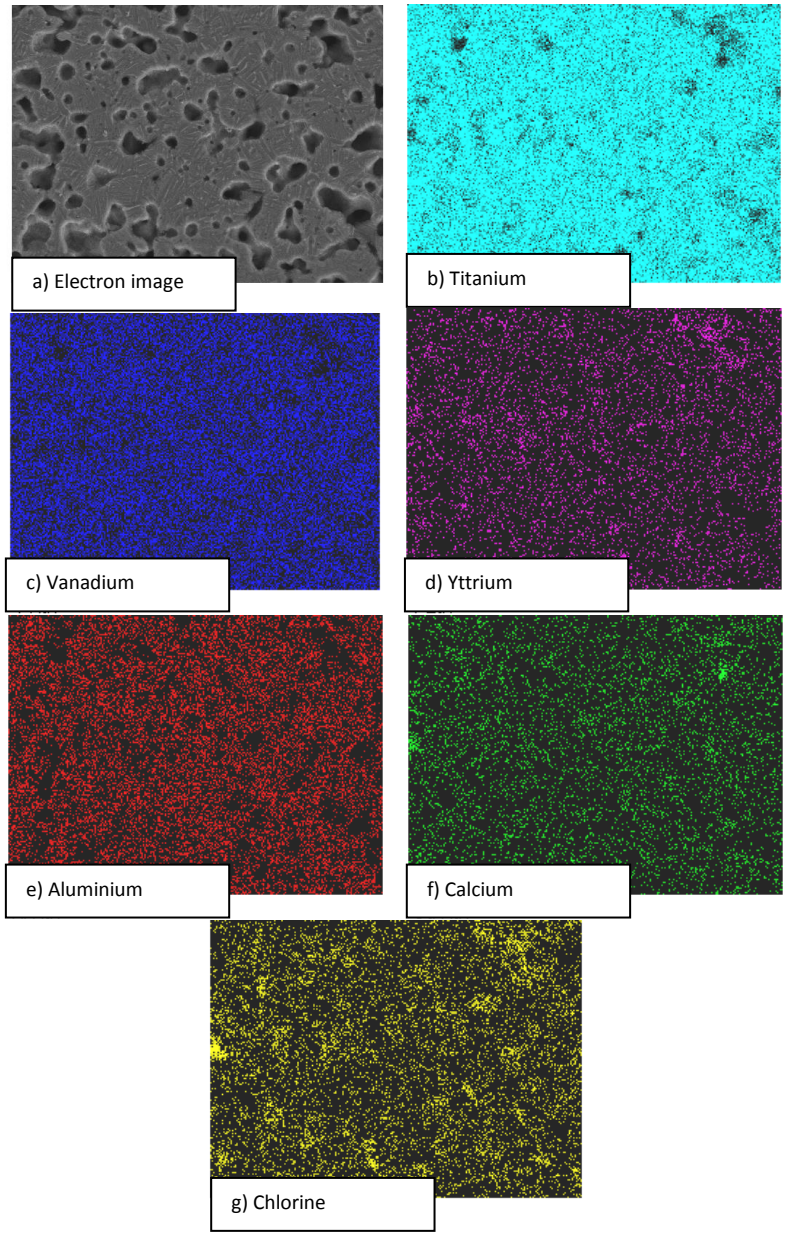

Figure 4.8: Elements mapping of Ti6Al4V-2Y.

From Figure 4.8, all elements of Ti6Al4V-2Y are well distributed across of the alloy. It was found that Y element is located mainly at the porous area and less located at the grain boundaries of the sample. An early conclusion can be made that different content of yttrium can changed element distribution.

4.4.3 Phase Identification of Ti6Al4V-7Y

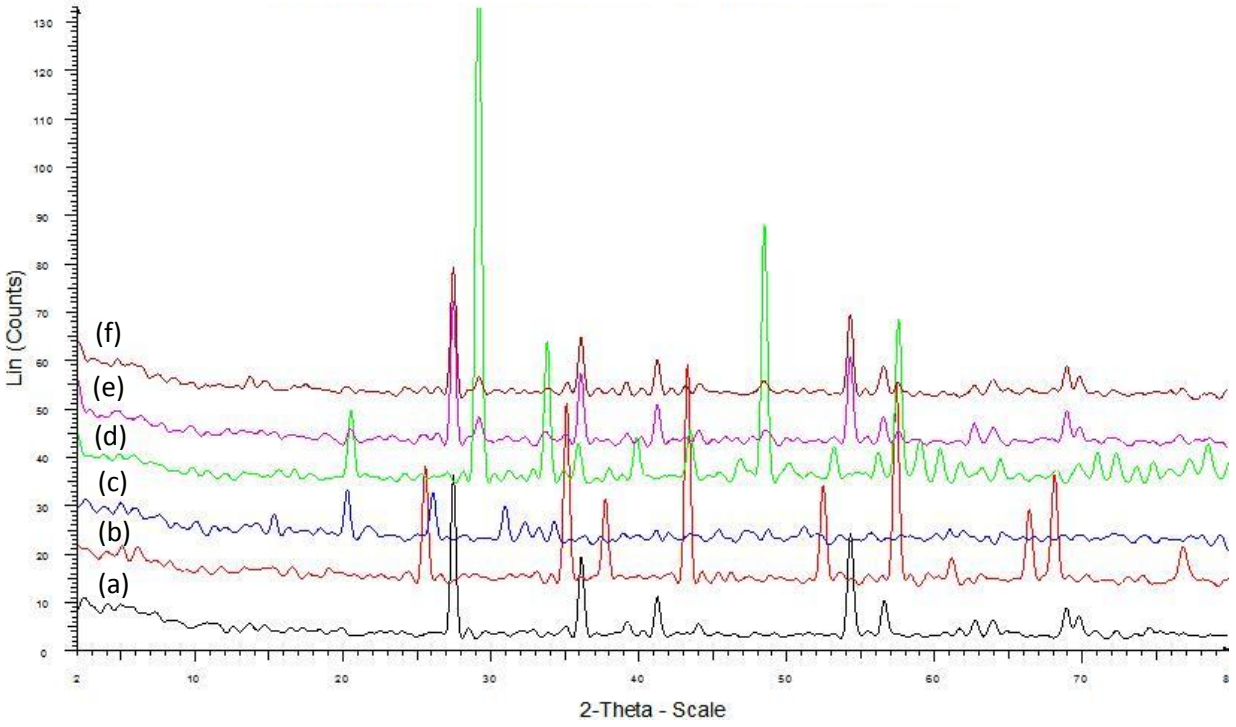

Figure 4.9: X-ray diffraction data for: a) TiO_2 powder b) Al_2O_3 powder c) V_2O_5 powder d) Y_2O_3 powder e) Ti6Al4V-7Y powder f) Ti6Al4V-7Y compressed at 2.4 tons powder.

The X-ray diffraction (XRD) patterns of Ti6Al4V-7Y powder, Ti-6Al-4V 7Y compressed and oxide powder of titanium alloy are shown in Figure 4.9. It was confirm that the crystal structure of Ti6Al4V-7Y and Ti6Al4V-7Y compressed at 2.4 tons powder are the same with TiO_2 powder because the diffraction peak is quite similar. 7% concentration of Y element resulted in a new compound of Y_2O_3. It is believed that the diffraction peak intensities of Y_2O_3 phases increased with the increasing of Y content, which indicated Y_2O_3 phase content increased steadily. Furthermore, the diffraction peak of Al_2O_3 and V_2O_5 were loss in Ti6Al4V-7Y and Ti6Al4V-7Y compressed patterns.

4.6 Discussion

Based on the results obtained from optical microscope, Various Pressure-Field Emission Scanning Electron Microscope, Vickers hardness test and X-ray diffraction, it can be seen that Ti6Al4V-2Y is strongest than Ti6Al4V-7Y. The grain size of Ti6Al4V-2Y is smaller than Ti6Al4V-7Y which leads to strong and increase in hardness properties of Ti6Al4V-2Y. Conclusion can be made that less content of Y element can reduce the grain size and provide better yield and hardness strength. Furthermore, all elements are well distributed across the samples but Y element is located mainly at the grain boundaries and less located at the porous area of the Ti6Al4V-7Y sample. On the other hand, Y element is located mainly at the porous area and less located at the grain boundaries of the Ti6Al4V-2Y sample. In this study we explore the use of the FFC Cambridge process to produce Ti6Al4V-7Y. A study conducted for the US Department of Energy in 2004 identified more than a dozen emerging technologies for Ti extraction. However, only the FFC Cambridge process lends itself to the production of Ti foams via the reduction of a porous TiO2 precursor [14]. The porosities in Ti6Al4V-7Y offer numerous advantages in biomedical applications. The function of porous structure can allow tissue in-growth and vascularization. Furthermore, the presence of porosity can lower the strength and satisfy the strength requirements for bone replacement in biomedical application [12]. It was proving that the crystal structure of Ti6Al4V-7Y and Ti6Al4V-7Y compressed at 2.4 tons powder are the same with TiO_2 powder because the diffraction peak is quite similar. Furthermore, different concentration of Y element in Ti6Al4V resulted in the diffraction peak intensities of Y_2O_3 phases. On the other hand, the diffraction peak of Al_2O_3 and V_2O_5 were loss in Ti6Al4V-7Y and Ti6Al4V-7Y compressed patterns.

CHAPTER 5

5. CONCLUSION AND RECOMMENDATION

5.1 Conclusion

As a conclusion, this project is a wide-ranging study and research upon the theory of pinning a foreign element into metal alloys and utilization of multiple types of optical observation apparatus and hardness tester. The data received from observation gave out the precise properties of the final result which is Ti6Al4V-7Y and it was compared with the final result of Ti6Al4V-2Y and literature reviews. Based on the results obtained from Vickers hardness test, it can be seen that Ti6Al4V-7Y has average hardness of 156.1 HV while average hardness of Ti6Al4V-2Y is 161.7 HV. From micrograph acquired, the average grain size of Ti6Al4V-7Y is 2.53μm and average grain size of Ti6Al4V-2Y is 1.44μm. Conclusion can be made that less content of Y element can reduce the grain size and provide better yield and hardness strength to the alloy. The porosities in Ti6Al4V-7Y offer numerous advantages in biomedical applications. The function of porous structure can allow tissue in-growth and vascularization. All elements are well distributed across the samples but Y element is located mainly at the grain boundaries and less located at the porous area of the Ti6Al4V-7Y sample. On the other hand, Y element is located mainly at the porous area and less located at the grain boundaries of the Ti6Al4V-2Y sample. It was proved that the crystal structure of Ti6Al4V-7Y and Ti6Al4V-7Y compressed at 2.4 tons powder are the same with TiO_2 powder because the diffraction peak is quite similar. Furthermore, different concentration of Y element in Ti6Al4V resulted in the diffraction peak intensities of Y_2O_3 phases. On the other hand, the diffraction peak of Al_2O_3 and V_2O_5 were loss in Ti6Al4V-7Y and Ti6Al4V-7Y compressed patterns. Overall, the objectives of determining mechanical and physical properties of Ti6Al4V-7Y and identifying the effect of different addition contents of wt.% Y element in the alloy were successfully achieved within the time frame given.

5.2 Recommendation

For the suggested future works, advance research on Ti6Al4V with additional content of Y element such as abrasive property, etc, is greatly encouraged because it can give better application in bio-medical.

REFERENCES

[1] Mohandas, Fray (2004). *FFC Cambridge Process and Removal of Oxygen from Metal-Oxygen System by Molten Salt Electrolysis: An Overview*, Trans. Indian Inst. Met. Vol. 57:6 [p. 579-592].

[2] Cao, Min, Wu, Xian, Shang (2006). *Pinning of grain boundaries by second phase particles in equal-channel angularly pressed Cu-Fe-P alloy*, Material Science & Engineering, Elsevier B. V [p. 86-91].

[3] Obasi, Birocsa, Fonseca, Preuss (2011) *Effect of β growth on variant selection and texture memory effect during α ->β ->α phase transformation in Ti 6Al-4V*, Acta Materialia, Elsevier [p. 1048-1058].

[4] Ti6Al4V Titanium Alloy, *29 June 2012 (retrieve from http://www.arcam.com/CommonResources/Files/Materials/Arcam-Ti6Al4V-Titanium-Alloy.pdf).*

[5] Lu, (2005). *Hydrogen Embrittlement of Aluminum: The Crucial Role of Vacancies*, The American Physical Society [p. 1-4].

[6] Fenn, Cooley, Fray, Smith (2004). *Exploiting the FFC Cambridge Process*, Advanced Materials & Processes, Metalysis Ltd. [p.51-53].

[7] Bhagat, Jackson, Inman, Dashwood (2008). *The Production of Ti-Mo from Mixed Oxide Precursors via the FFC Cambridge Process*, Journal of The Electrochemical Society.

[8] Bhagat, R. et al (2010). *In-Situ Synchrotron Diffraction of the Electrochemical Reduction Pathway of TiO_2,* Acta Materialia, vol. 58:15, [p. 5057-5062].

[9] Alloy Data Titanium Alloy Ti 6Al-4V, 27 June 2012 *(retrieve from http://www.cartech.com).*

[10] Vickers Test, 11 August 2012, *(retrieved from http://www.instron.us/wa/applications/test_types/hardness/vickers.aspx).*

[11] X-ray Diffraction (XRD), 1 July 2012, *(retrieved from http://web.pdx.edu/~pmoeck/phy381/Topic5a-XRD.pdf).*

[12] Egemen Akar (2005). *Processing and mechanical testing of Ti6Al4V foams for hand tissue implant applications,* Izmir Institute of Technology.

[13] Wang, Ma, Nie, Wang, Shang (2012). *Effects of Y addition on microstructure and mechanical properties of TiC/Ti6Al4V composites*, Material Science & Engineering, Elsevier [p. 242-248].

[14] Singh, Lee, Jones, Poologasundarampillai, Post, Lindley, Dashwood (2010). *Hierarchically structured titanium foams for tissue scaffold applications*, Acta Biomaterialia 6, Elsevier [p. 4596-4599].